Gleaning meaningful information from seismic attributes

Satinder Chopra[1]* and Kurt Marfurt[2]

Abstract

Seismic attributes form an integral part of most of today's interpretation projects. Attributes enhance subtle features in the seismic data that may otherwise be overlooked or require a great deal of time to map. The quality of attribute displays is directly proportional to the quality of the input seismic data. Ideally, all amplitude, phase, and travel time distortion effects due to near-surface and overburden heterogeneities as well as those introduced by acquisition and processing should be optimally handled, even if they cannot be totally eliminated. In practice, even with careful acquisition, processing, and imaging, our data will still exhibit a certain level of noise. We show how structure-oriented filtering can eliminate random noise, with the principal component filter providing better results than the more familiar mean and median filters. The acquisition footprint is a form of coherent, rather than random, noise and requires a different filtering approach, ideally in the prestack domain prior to stacking. Finally, we show that different implementations of a given attribute can make a difference, with energy ratio coherence providing more robust images than semblance. We illustrate these findings through application to a suite of examples from Alberta, Canada.

Introduction

With the exception of AVO and anisotropic velocity analysis, all attribute work is done on data that have been migrated. Such seismic data volumes are usually contaminated by both random and coherent noise, even when the data have been migrated reasonably well and are multiple-free. For seismic attributes to do a good job, the input seismic data need to be free of noise. From the interpreter's point of view, there are two types of noise — noise which the interpreter can address through applying some relatively simple processes to the migrated data volume, and noise which requires reprocessing of the prestack data. The interpreter can address noise spikes, a limited degree of migration operator aliasing, small velocity errors, and backscattered noise that can result in acquisition footprint, and random noise through bandpass, k_x-k_y, and structure-oriented filtering. In contrast, significant velocity errors will result in overlapping reflector signals that produce discontinuity and tuning artifacts which may overwhelm corresponding events associated with the subsurface geology. Surface and interbed multiples result in similar strong artifacts. Our experience has been that if reflection events are highly ambiguous, as they commonly are subsalt, then attributes have only limited value. While the interpreter can play a crucial role in identifying primaries and estimating velocities through integrating well control and geological models, fixing the prestack data requires that the data be sent back to a processing team.

Marfurt et al. (1998) demonstrated the use of an accurate 3D dip filter for removal of steeply dipping noise. While the filtered result looks cleaner and the resulting attribute image is more continuous, there is always the danger of removing signal by filtering and so application of such a filter may be discouraged for cases where mapping fractures or other subtle discontinuities are the objective. Gulunay et al. (1993) and Linville and Meek (1995) designed dip filters that first estimated the dip of the most coherent noise event and then subtracted it in a least-squares sense from the data. Done (1999) used a principal component filter to achieve the same result. Fomel (2002) used prediction error filters to design a plane-wave destructor to reduce aliased noise. Clearly, a close relationship exists between geometric attributes and coherent noise estimation and subtraction. The criterion for successfully applying these kinds of filters to migrated data volumes is to avoid smoothing across faults and other discontinuities.

We begin our discussion by reviewing alternative means of suppressing random noise on our migrated seismic images, with the most promising methods being various implementations of structure-oriented filtering. Next, we address acquisition footprint, which may appear to be random in the temporal domain but is highly correlated to the acquisition geometry in the spatial domain. After data preconditioning, we evaluate alternative algorithmic implementations for both coherence and curvature computation. At each step, we illustrate the impact of these filters and algorithmic choices on data volumes acquired in Alberta, Canada. We conclude with a summary of limitations and recommendations as to which kinds of noise can be suppressed in the post-migration domain by an experienced interpreter, and which kinds of noise require prestack processing in a data processing centre.

[1] *Arcis Corporation, 2600, 111-5th Avenue SW, Calgary, Alberta, Canada T2P 3Y6.*
[2] *ConocoPhillips School of Geology and Geophysics, University of Oklahoma, 100 East Boyd Street, Norman, OK 73019, USA.*
**Corresponding author, E-mail: schopra@arcis.com*

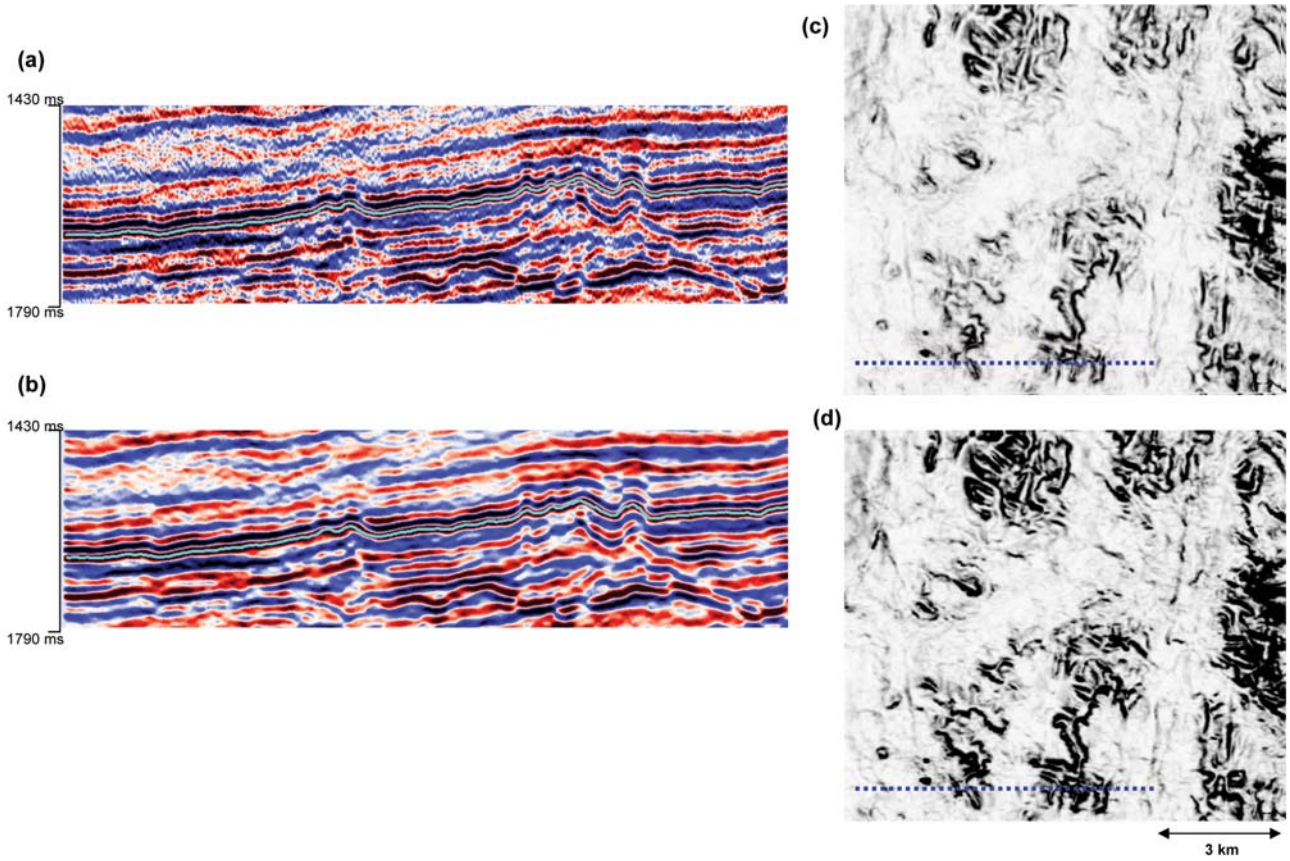

Figure 1 *Segment of a seismic section (a) before and (b) after application of a 3 x 3 dip-steered median filter. Horizon slices through coherence volumes run on (c) the input seismic volume, and (d) the median filtered seismic volume, 76 ms below the horizon highlighted in (a) and (b). (Data courtesy of Arcis Corporation, Calgary).*

Suppression of random noise

Mean, alpha-trimmed mean, and median filters are commonly used during processing to suppress random noise. A more desirable application would be of a dip-steered mean or median filter, which has the effect of enhancing laterally continuous events by reducing randomly distributed noise without wiping out structural reflection detail. The filter picks up samples within the chosen aperture along the local dip and azimuth and replaces the amplitude of the central sample position with the median value of the amplitudes. The median filter can also be applied iteratively, reducing random noise at each successive iteration, but will not significantly increase the high frequency geological component of the surface. Figure 1 shows a segment of a seismic section before (Figure 1a) and after (Figure 1b) application of a 3 × 3 median filter. Notice the cleaner background and the focused amplitudes of the seismic reflections after median filtering. Attributes run on median-filtered data exhibit cleaner-looking features as well as background. Figures 1c and d show horizon slices from the coherence volumes generated before and after median filtering. The noise in the background has been toned down after median filtering, and the features are somewhat more coherent. The patchy low coherence features correspond to Devonian reefs that grew in phases, as indicated by the almost vertical gaps between these features.

Structure-oriented filtering

While dip-steered mean or median filters and alpha-trimmed mean filters work on seismic data, they may also smear fault information as well as marginally lowering the frequency content of the data. Hoecker and Fehmers (2002) addressed this problem by using an 'anisotropic diffusion' smoothing algorithm. The diffusion part of the name implies that the filter is applied iteratively, much as an interpreter would apply iterative smoothing to a time-structure map. Most important, no smoothing takes place if a discontinuity is detected, thereby preserving the appearance of major faults and stratigraphic edges. Luo et al. (2002) proposed a competing method that uses a multiwindow (Kuwahara) filter to address the same problem. Both approaches use a mean or median filter applied to data values that fall within a spatial analysis window with a thickness of one sample.

Marfurt (2006) described a multiwindow (Kuwahara) principal component (pc) filter that uses a small volume of data samples to compute the waveform which best represents the seismic data in the spatial analysis window. Seismic processors may be more familiar with the pc filter as equivalent to the Karhunen-Loève (KL) filter. Figure 2 shows a comparison of vertical before and after pc filtering on a seismic data set from Alberta. Notice not only the overall cleaner look of the section after pc filtering, but also the sharpening of the vertical

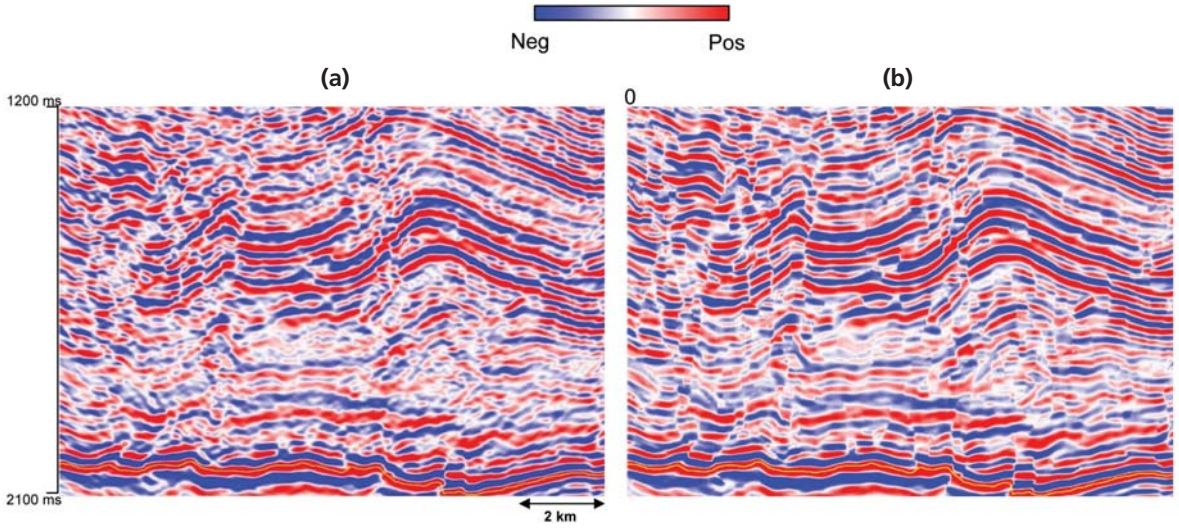

Figure 2 *Seismic data (a) before and (b) after structure-oriented filtering. (Data courtesy of Olympic Seismic, Calgary).*

faults. The filter was applied iteratively three times such that the end result depends on 49 neighbouring traces.

Figures 2a and b use 99 overlapping windows each of which consists of 9 traces and 11 samples (± 10 ms) parallel to the dip/azimuth at the centre of each window. We then apply our pc filter to the analysis point using the window that contains the most coherent data. Because it uses more data (for our example, 11 times more), the pc filter in general produces significantly better results than the corresponding mean and median filters. Notice the sharpened faults as well as the overall reduced background noise level. In Figure 3 we show segments of seismic sections from the input seismic data (Figure 3a), the data filtered with a 3 × 3 dip-steered median filter, which is sufficient in many cases (Figure 3b), and the data filtered with a 9-point dip-steered pc filter (Figure 3c). Notice that the amplitude levels in the highlighted zones are somewhat reduced after median filtering, but remain unchanged after pc filtering.

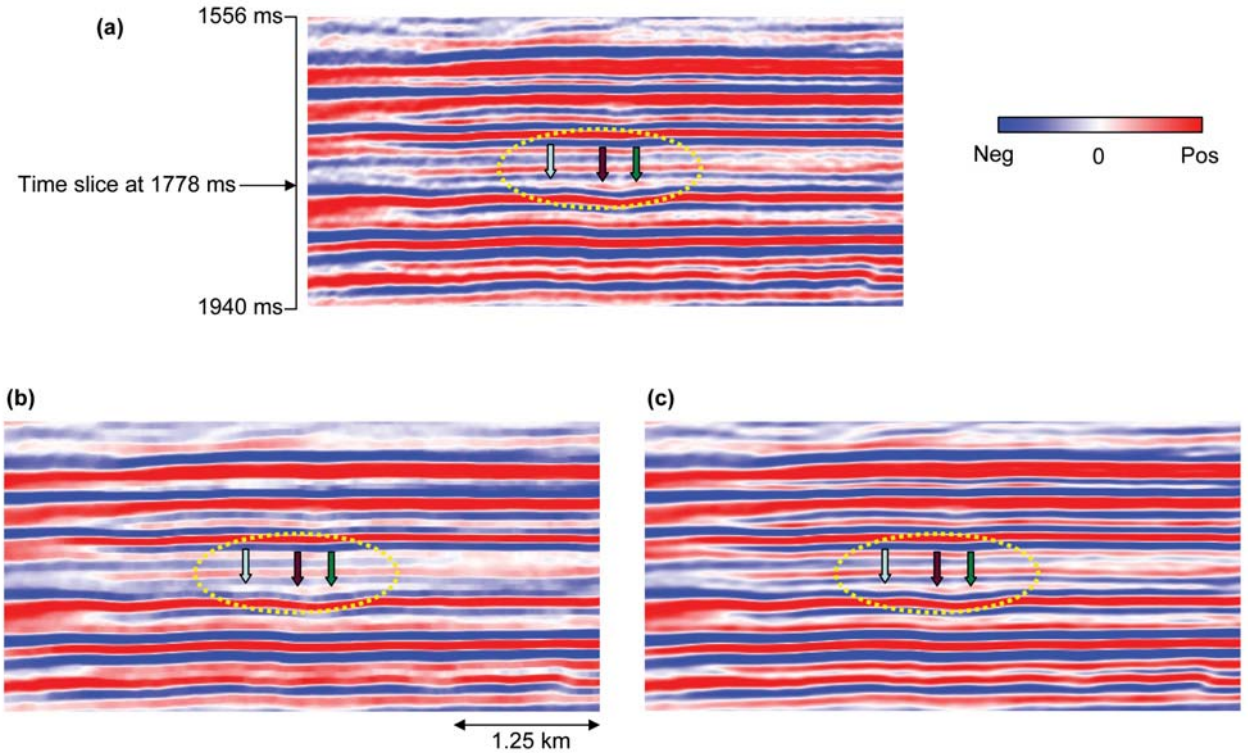

Figure 3 *Segments of seismic sections from (a) input data, (b) input data passed through a dip-steered 3 x 3 median filter, and (c) input data after pc filtering. Notice that amplitude levels in the highlighted zones are somewhat reduced after median filtering, but remain unchanged after pc filtering. (Data courtesy of Arcis Corporation, Calgary).*

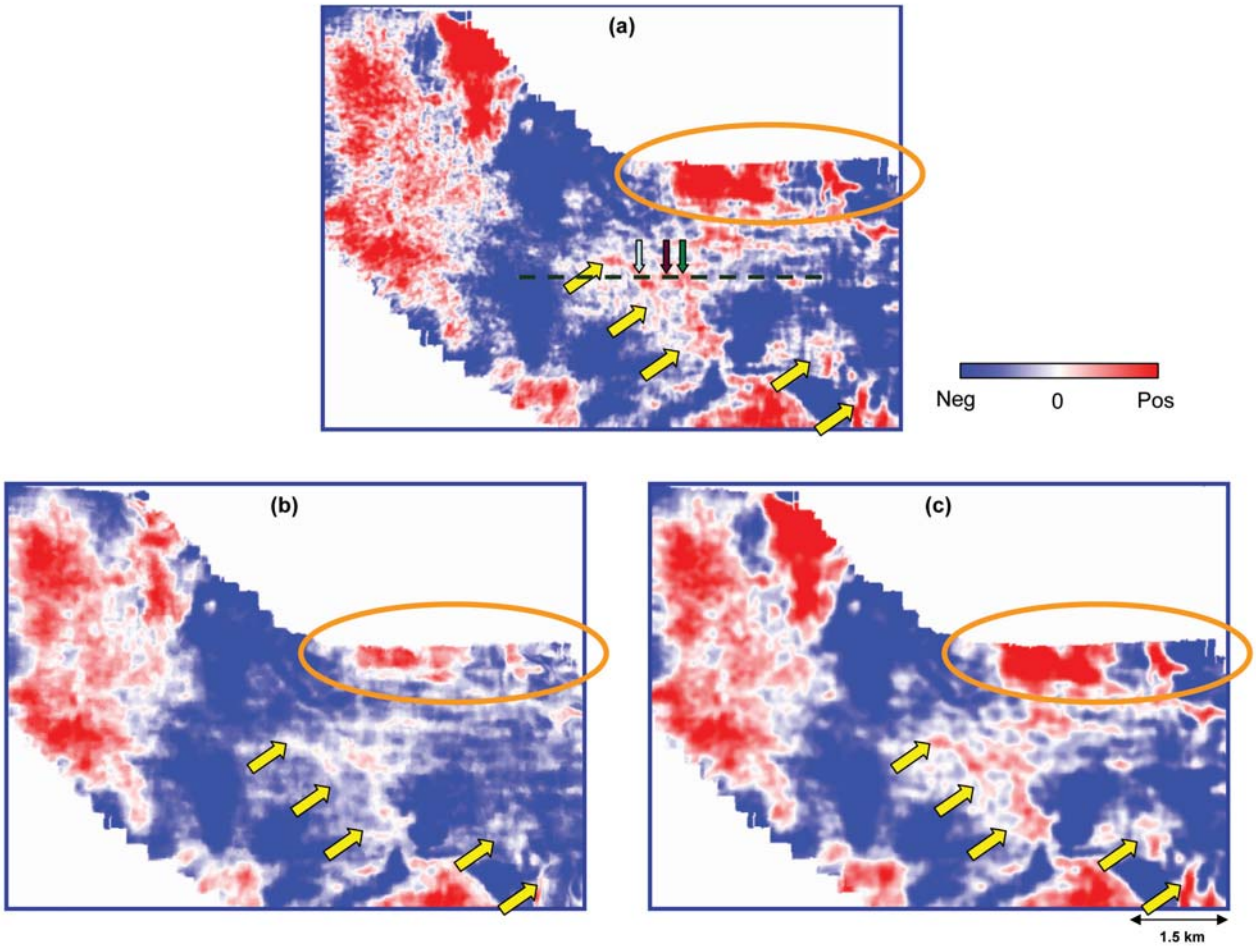

Figure 4 *Time slices at 1778 ms through (a) a seismic data volume, (b) the seismic volume in (a) subjected to a 3 × 3 dip-steered median filter, and (c) the seismic volume in (a) subjected to pc filtering. (Data courtesy of Arcis Corporation, Calgary).*

Figure 4 shows a comparison of time slices from the same three data sets, the input seismic data (Figure 4a), the seismic data filtered with a 3 × 3 dip-steered median filter (Figure 4b), and the seismic data filtered with a 9-point dip-steered pc filter (Figure 4c). Notice, as shown in the highlighted ellipses, that the pc-filtered display follows the features more closely on the time slices than the median filtered display does. Similarly, the yellow arrows on the pc-filtered display show up a pattern in red similar to the input, but the median filtered output shows a weakening of amplitudes on those features. Figure 5 shows a comparison along a phantom horizon slice 66 ms above a marker horizon. Again notice in the highlighting ellipses and the trapeziums, as indicated with the arrows, how on the pc-filtered display the event features follow similar features on the input data, except now they look somewhat more focused. The median filtered output looks different and so is unacceptable. Improved event focusing and reduced background noise levels after structure-oriented filtering are clearly evident.

We advise the hopeful reader that there is no such thing as a 'silver bullet' in seismic data processing. If the data are contaminated by high-amplitude noise spikes, then a median, alpha-trim mean, or other non-linear filter will provide superior results. Likewise, while the pc filter will preserve amplitude variations in coherent signal, it may exacerbate acquisition footprint amplitude artifacts, whereas a mean filter will smooth them out. Structure-oriented filtering also exacerbates the fault shadow problem, which should properly be addressed through depth migration.

Acquisition footprint suppression

Acquisition footprint is a term we use to define linear spatial grid patterns seen on 3D seismic time slices. These patterns are commonly seen on shallow time slices or horizon amplitude maps as striations masking the actual amplitude anomalies under consideration for stratigraphic interpretation, AVO analysis, and reservoir attribute studies (Marfurt et al., 1998). An acquisition footprint may be present due to various reasons, but two general types of footprint can be distinguished: those depending on the details of the acquisition geometry, and those arising from signal processing problems (Drummond et al., 2000).

The choice of any acquisition design is characterized by a particular distribution of fold, offset, and azimuth. Apart from

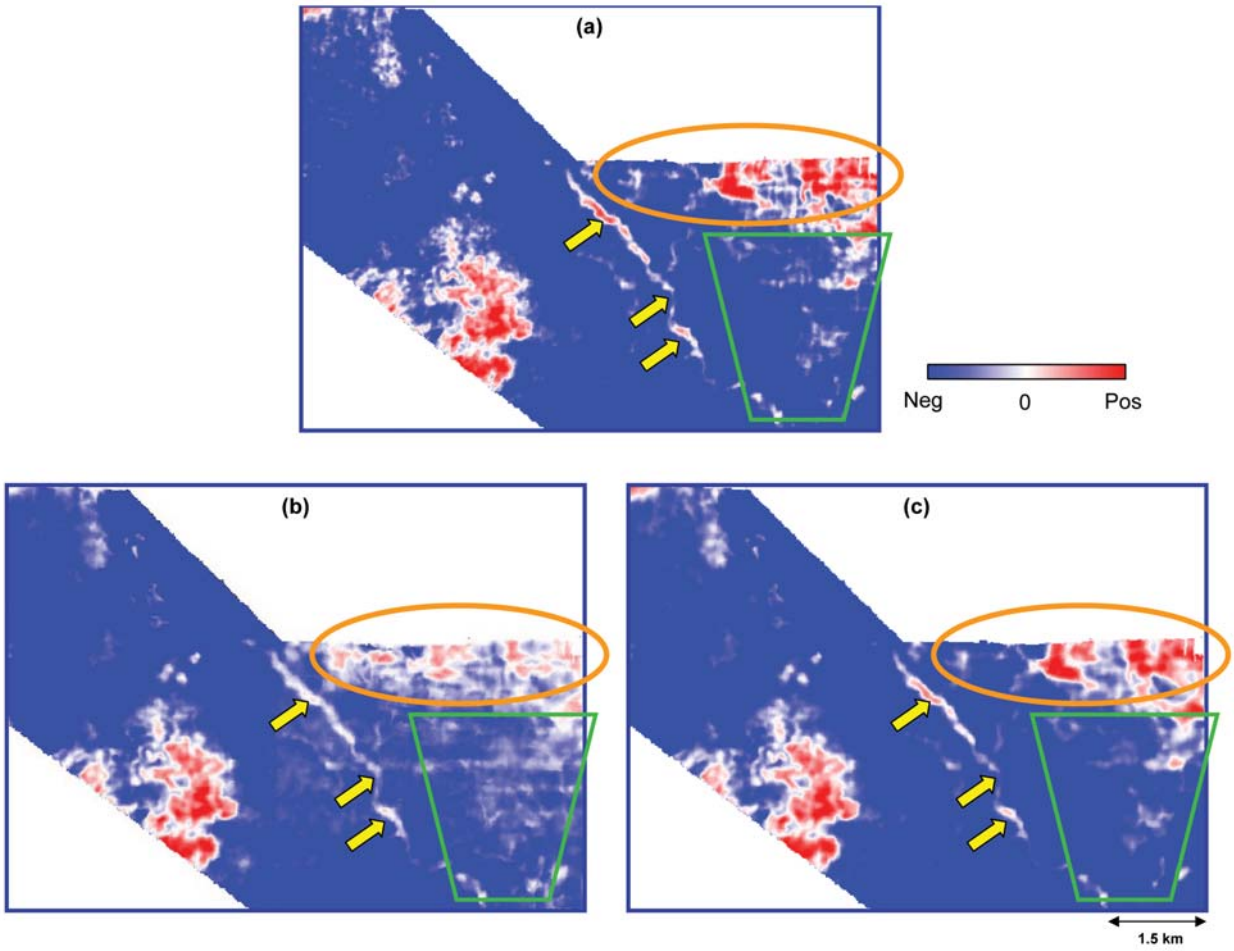

Figure 5 *Horizon slices 66 ms below a flattened marker through (a) the input seismic volume, (b) the input seismic volume subjected to a 5 × 5 dip-steered median filter, and (c) the seismic volume in (a) subjected to pc filtering. (Data courtesy of Arcis Corporation, Calgary).*

some variation in the taper zone, the fold for most common geometries is uniform for all seismic bins. However, the offset and azimuth distribution can vary from bin to bin, or can be uniform in the inline direction and irregular in the cross-line direction.

Such variations can lead to undesirable effects on the reflected signal. Deviations from a regular geometry pattern, such as inaccessible patches within a 3D survey area that are under human habitation or the location of a power station, can be responsible for such variation. Other examples of factors that affect the offset and azimuth distribution are azimuthally biased receiver array responses, suppressing inline noise but passing cross-line noise, and malfunctioning of the recording system. Cable feathering resulting from strong water currents and undershooting of obstructed areas are examples in the marine environment.

Very often economic considerations compel coarse sampling in 3D data acquisition, which can cause artifacts during processing. Coarse spatial sampling leads to aliasing, and aliased steeply dipping noise resulting from ground roll or multiples, for example, creates artifacts. Aliased noise can be accentuated during processing and leak into the stack volumes as spatially periodic events, forming an acquisition footprint. Other processes that tend to accentuate footprints are residual NMO caused by incorrect velocities, systematic errors in computed offsets, or amplitude variations caused by inadequate 3D DMO formulation (Walker et al., 1995; Budd et al., 1995), 3D prestack migration, signal enhancements based on *f-x-y* random noise attenuation, and coherency filtering (Moldoveanu et al., 1999).

An acquisition footprint, whether resulting from acquisition design or accentuation during processing, is a nuisance for the interpreter. Efforts are sometimes made to prevent accentuation of the footprint during processing, usually by adopting interpolation or extrapolation to remedy the 'sparseness' of the input data volumes before applying multi-channel processes. If interpolation is computationally prohibitive, we can resort to trace mixing, which tends to minimize the footprint effect at the risk of reducing lateral resolution. Gulunay (1999) found that wavenumber domain filtering based on the acquisition design often works. A similar filtering method for non-orthogonal geometries has been suggested by Soubras (2001).

Chopra and Larsen (2000) suggested a similar way of dealing with the acquisition footprint, which is to analyze the

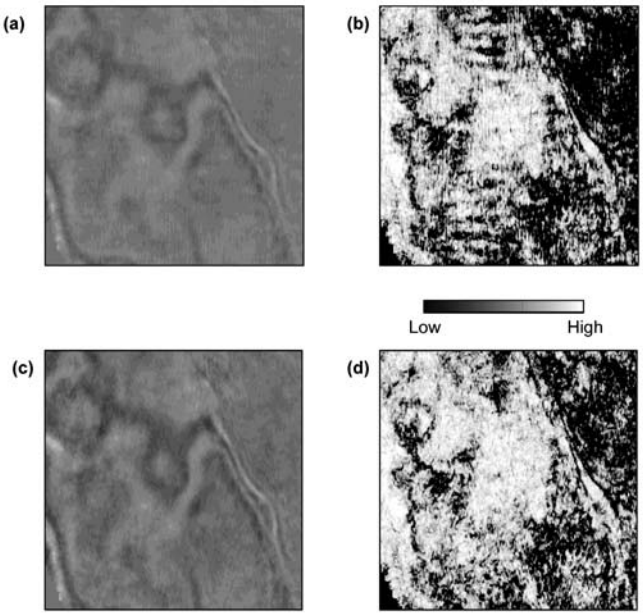

Figure 6 *Time slices at 1316 ms through (a) a seismic data volume and (b) the corresponding coherence volume. (c) Time slice equivalent to the seismic slice in (a) from the seismic volume subjected to acquisition footprint filtering, and (d) equivalent slice from the coherence volume generated from the filtered seismic volume in (c).*

footprint-contaminated post-stack migrated data, time slice by time slice, in the k_x-k_y wavenumber domain. By animating through the seismic as well as the corresponding coherence slices, the interpreter can define the change in footprint with depth. Figure 6 shows time slices at 1316 ms where the acquisition footprint shows up prominently on the coherence slice as striations in the E-W and N-S directions in Figure 6b, masking the seismic reflections. The coherence slices were transformed into the k_x-k_y domain and a filter was designed manually at intervals of 100 ms. Interpolation between these filters yielded one k_x-k_y filter for each time slice, and these filters were applied to the original seismic data. The equivalent time slice from the coherence volume derived from the seismic volume after k_x-k_y filtering (Figure 6d) shows that the seismic volume is clear of any footprint lineations and represents a significant improvement in data quality that will lead to more confident interpretation.

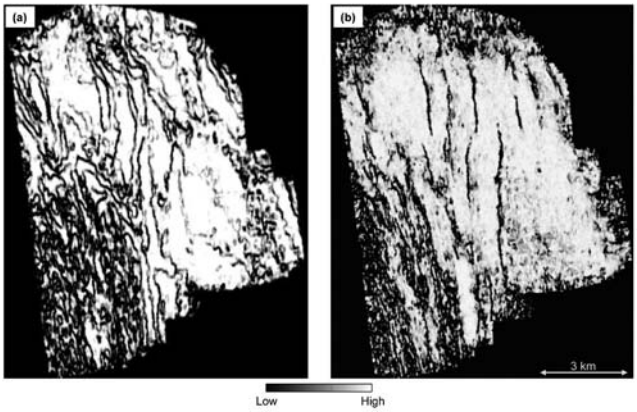

Figure 7 *Time slices through a coherence volume computed (a) without and (b) with dip-steering. (Data courtesy of Olympic Seismic, Calgary).*

Apart from k_x-k_y filtering, spatially adaptive methods using wavelet transforms have been suggested for highly irregular footprint (Jervis, 2006; Cvetkovic et al., 2007). Al-Bannagi et al. (2005) proposed a method using principal component analysis.

Algorithmic implementation

Dip-steering option during computation of geometrical attributes

Estimation of coherence is often done under the assumption of flat events, i.e., by disregarding dip. For data with dipping reflection events, this leads to misleading results. Because coherence algorithms based on semblance, variance, or eigen-decomposition typically include many traces about the desired output location, the local reflector dip and azimuth should be computed as a first step. Both semblance and variance estimates of coherence of seismic data are currently provided as options on commercial interpretation workstations. In the interest of computational efficiency, dip-steering options are either not provided or are not robust enough to handle the computational accuracy. A good workflow would involve a direct search of volumetric dip and azimuth prior to, or as part of, the coherence calculations. This could be 50–200 times more intensive computationally than a coherence calculation without a dip-steering option. Such computations are usually implemented on clusters in a processing centre. In such a scenario, the interpreter loads a precomputed coherence volume that includes an explicit volumetric dip and azimuth search and then extracts either time slices or horizon slices. Coherence algorithms based on the gradient structure tensor (Randen et al., 2002), such as the chaos and related attributes, do search for similarity along structural dip; however, their analysis window is usually oriented along the acquisition and time axes.

Figure 7 shows time slices from two different coherence volumes. On the left is a time slice from a coherence volume generated without the dip-steering option. Note the artifacts (sometimes called structural leakage) following structural contours on the coherence image that complicate interpretation. On the right the same time slice is shown after correctly calculating coherence along a non-zero estimate of dip/azimuth. We now see the faults clearly, uncontaminated by structural artifacts.

In the absence of a robust dip-search coherence algorithm, the interpreter should first extract a slab of the seismic volume about an appropriately smoothed interpreted horizon, implicitly defining a dip/azimuth for each trace. The interpreter then needs to calculate coherence by invoking the dip-steering option on the flattened slab of data. This procedure could compromise results where no prominent horizon exists close to the zone of interest and where the geology does not follow such a reflector above or below. For careful reservoir characterization studies, a workflow with a robust dip-search coherence algorithm is recommended.

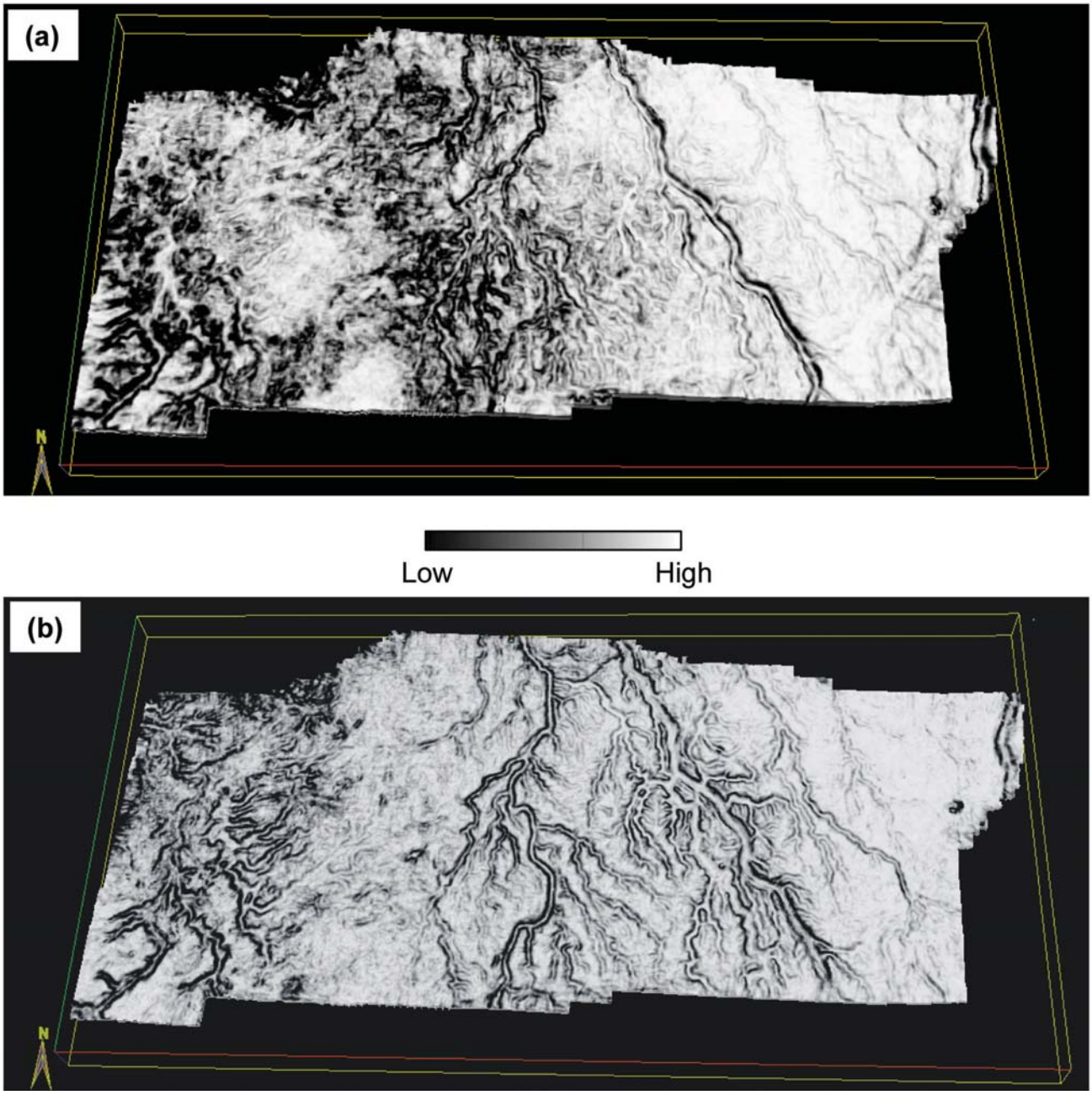

Figure 8 *Horizon slice through (a) coherence volume generated using a semblance algorithm directly on input data, and (b) coherence volume generated using energy ratio coherence algorithm run on pc-filtered seismic data. (Data courtesy of Arcis Corporation, Calgary).*

Choice of algorithms

Each of the alternative coherence algorithms have specific assumptions and consequently have different limitations. Algorithms based on cross-correlation (Bahorich and Farmer, 1995), eigen-decomposition of covariance matrices using eigenvalue ratios (Gersztenkorn and Marfurt, 1999), and gradient structure tensors (Randen et al., 2000) are sensitive to lateral changes in waveshape, and relatively insensitive to lateral changes in amplitude. Luo et al. (1996, 2005) have developed Sobel-filter like attributes that are primarily sensitive to lateral changes in amplitude, though obviously the waveform cannot change without changing the amplitude at any given sample. Perhaps the most commonly used algorithms are based on either an L2 implementation (Marfurt et al., 1998) or an L1 implementation of semblance, or on normalized variance, which are sensitive to both lateral changes in waveform and amplitude. In this paper we compute a covariance-based algorithm formed from analytic traces (the original data and its Hilbert transform). Rather than estimate coherence as the ratio of the largest eigenvalue to the sum of all the eigenvalues, we take the ratio of the energy of the coherent component of the analytic trace to the energy of the original analytic trace. We compute the coherent component of the analytic trace by projecting the original data onto the

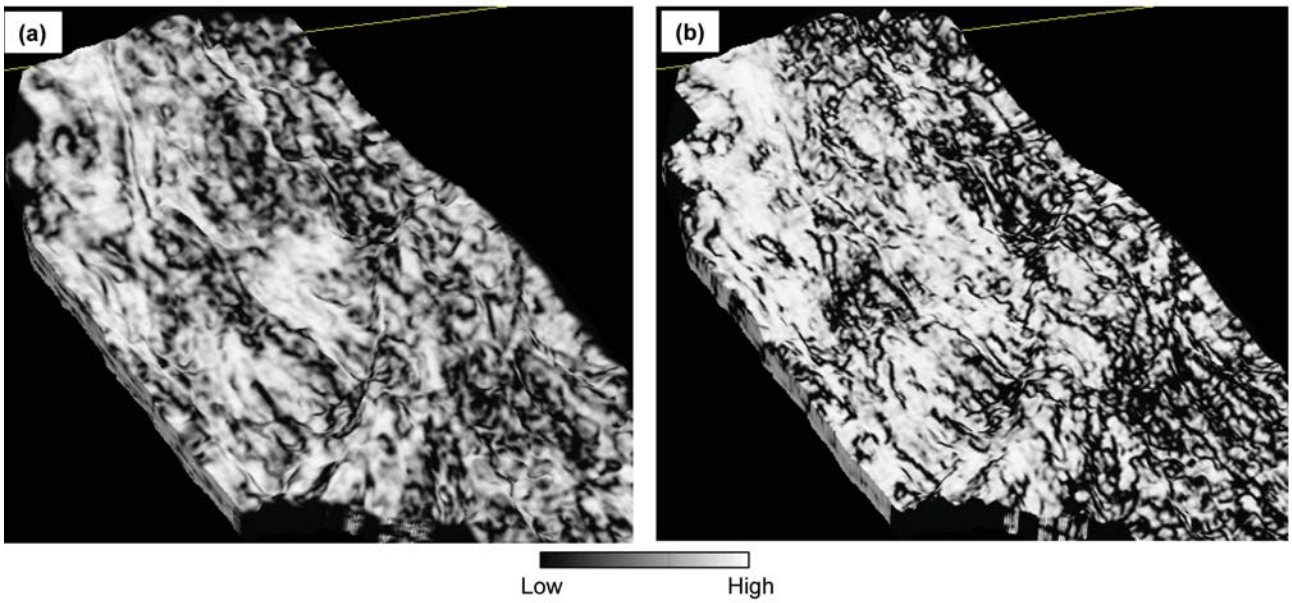

Figure 9 *Horizon slices through (a) coherence volume generated using a semblance algorithm directly on input data, and (b) coherence volume generated using energy ratio coherence algorithm run on pc-filtered seismic data.*

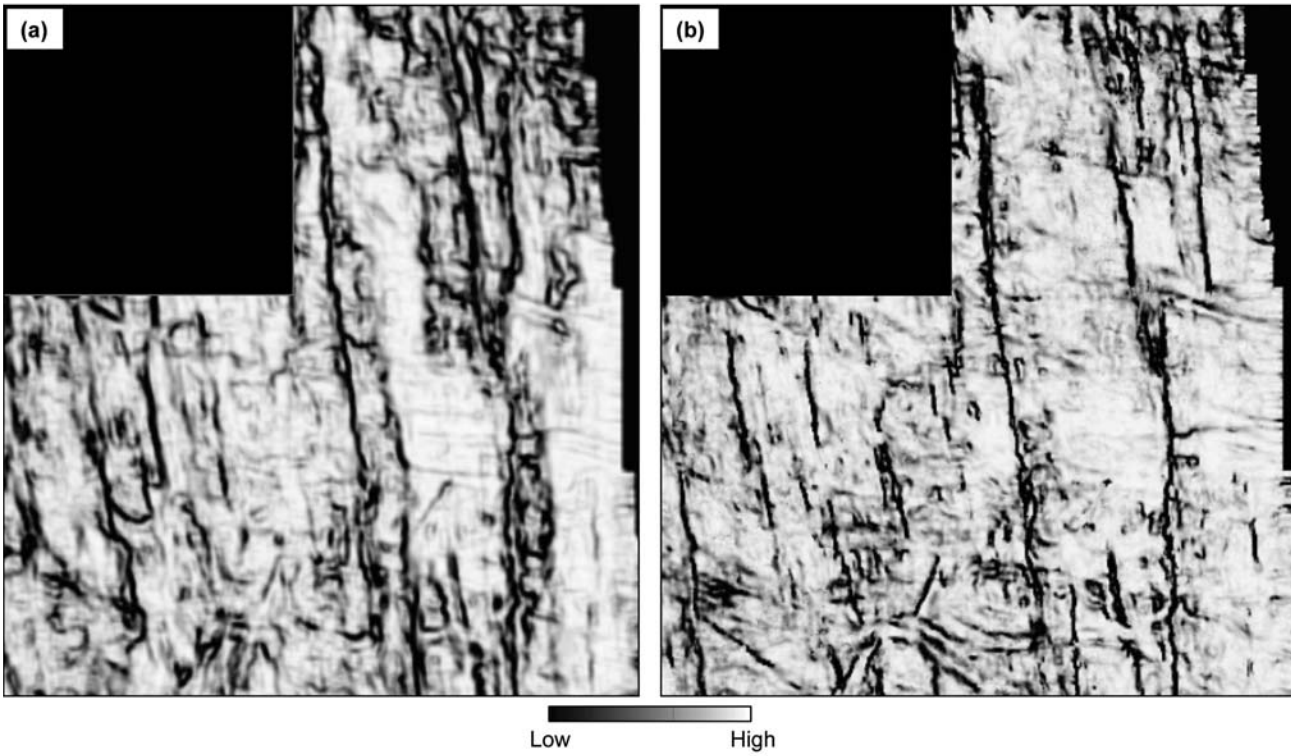

Figure 10 *Time slices through (a) coherence volume generated using a semblance algorithm directly on input data, and (b) coherence volume generated using energy ratio coherence algorithm run on pc-filtered seismic data.*

first eigenvector of the covariance matrix (the same process used in KL-filtering).

A further difference is that the computation is carried out on the analytic trace rather than on the real trace, thus avoiding artifacts near zero-crossings on the real trace.

Figure 8 shows a comparison between a 'conventional semblance' horizon slice from northeast British Columbia, Canada and the equivalent slice from the dip-steered energy ratio coherence volume run on the pc-filtered data, both computed using similar lateral and temporal parameters. Notice the clear definition of the main channel, running almost north-south, and also the branching channels, especially the ones to the left. A similar comparison of horizon slices from northern Alberta is shown in Figure 9.

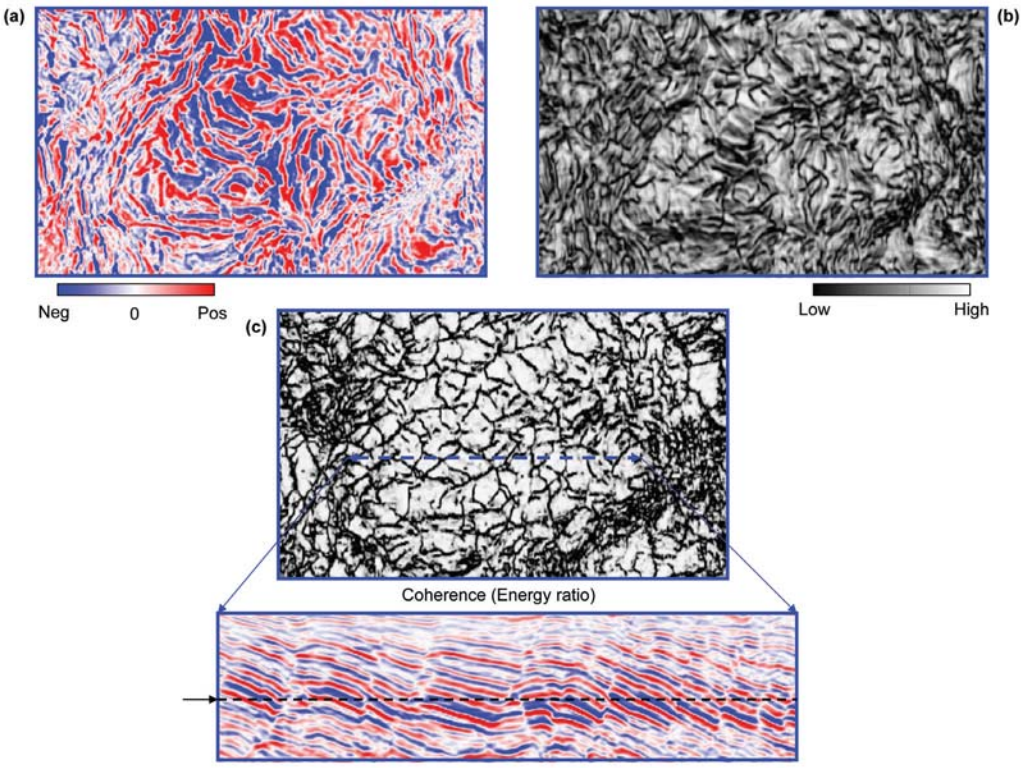

Figure 11 *Time slice at 1240 ms through (a) seismic amplitude, (b) semblance coherence, and (c) energy ratio coherence chair display from a data volume from the North Sea. The chair display helps correlate the fault breaks with their seismic signatures. (Data courtesy of Oilexco, Calgary).*

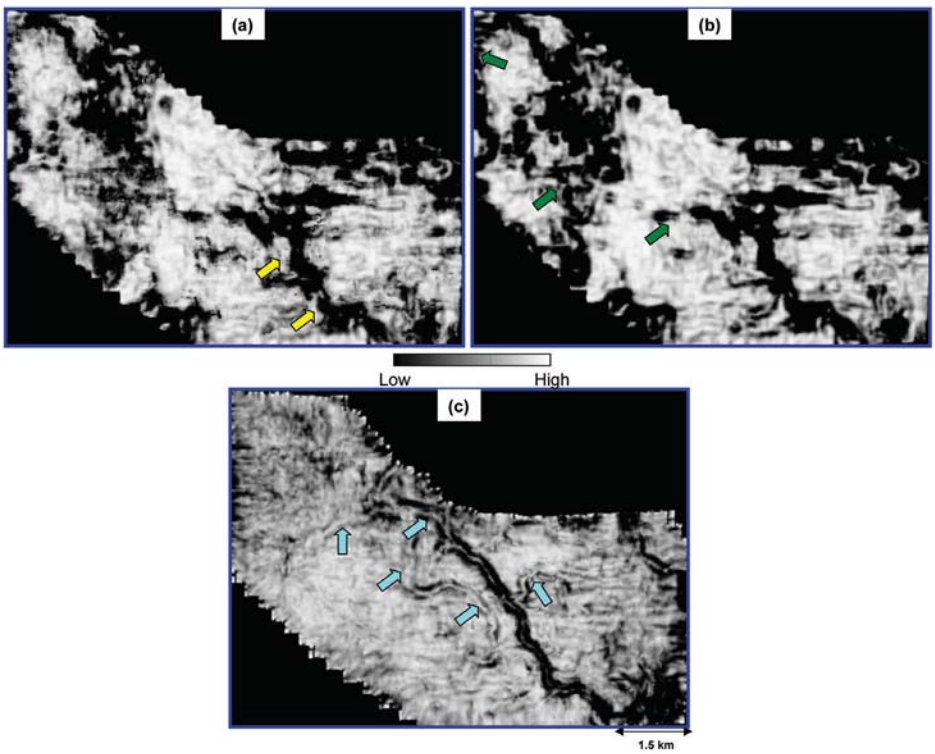

Figure 12 *Time slices through (a) coherence generated using a semblance algorithm directly on the input seismic data, (b) coherence generated using a semblance algorithm on the input seismic data which was median filtered, (c) coherence generated using energy ratio coherence algorithm on pc-filtered seismic data. (Data courtesy of Arcis Corporation, Calgary).*

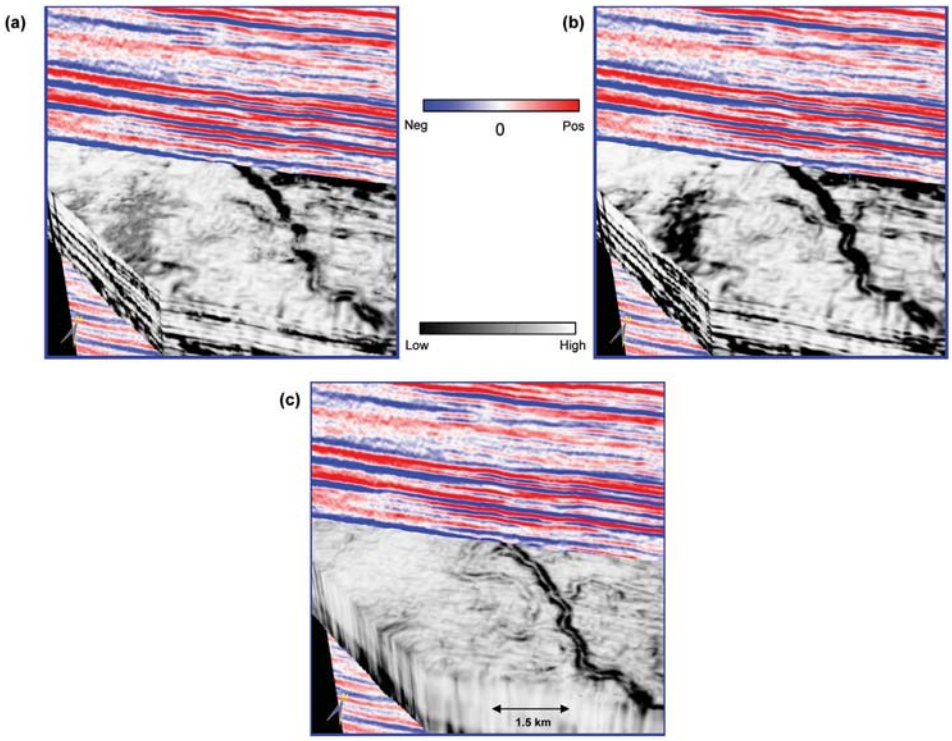

Figure 13 *Correlation of a seismic inline with horizon slices 66 ms below a flattened marker through (a) semblance coherence volume, (b) semblance coherence generated from median filtered seismic data, (c) energy ratio coherence volume generated from pc-filtered seismic data. (Data courtesy of Arcis Corporation, Calgary).*

Again, notice the clarity with which the faults/fractures are seen.

Figure 10 shows a comparison of time slices from a semblance volume (without the dip-steering option) and the energy ratio coherence volume with dip-steering on data that has been pc-filtered. Notice the crisper definition of faults and fractures in Figure 10b as compared with Figure10a.

Figure 11 depicts another comparison of a seismic time slice (1240 ms) from the North Sea area with equivalent time slices from the semblance coherence volume (Figure 11b) and a dip-steered energy ratio coherence volume run on pc-filtered seismic data (Figure 11c). Notice the clarity with which the polygonal faults stand out as well as the fractured zones (indicated with arrows) in Figure 11c. On the workstation, the individual polygonal faults can be correlated with their seismic signature by using the cursor-connect option, and are shown in the lower part of Figure 11c.

In Figure 12a we show time slices at 1778 ms from a semblance coherence volume from central Alberta. Notice the low-coherence features on the channel, indicated by the yellow arrows. There are other low-coherence features which are not so easily interpreted. The equivalent time slice from a semblance coherence volume obtained from the data after dip-steered median filtering is shown in Figure 12b. There is slightly better focusing of the low-coherence events of interest (indicated by green arrows).

In Figure12c we show the equivalent slice from energy ratio coherence volume generated from pc-filtered seismic data. Notice that not only does the NW-SE channel shows up clearly, but there are other thin channels (indicated by cyan arrows) which show up clearly on this display. Finally, in Figure 13 we show the correlation of horizon slices from these three coherence volumes 66 ms below a flattened marker with inline from the seismic volume. Notice that NW-SE channel now shows up on the semblance strat cubes in Figure 13a and b, but the clarity is not as good as in Figures 13c.

Conclusions

We have analyzed three important considerations for computation of geometrical attributes taking the coherence attribute as an example. These three considerations are (1) data conditioning, (2) using the dip-steering option for data with reflector dips, and (3) the choice of algorithm. We show that structure-oriented filtering run on seismic data sharpens the subsurface features of interest and tones down the background noise. The coherence attribute generated on such seismic volumes yields crisper features. Dip-steering options when used in coherence computation result in clearer looking volumes that are devoid of any structural contour patterns and so prevent misleading interpretation. Finally, a coherence algorithm based on the method of eigen-decomposition of covariance matrices, called the energy ratio method, demonstrates superior performance over other available algorithms. These three considerations, when adhered to in conjunction, yield superior displays for interpretation and should be embraced by seismic interpreters.

In today's rapidly expanding interactive interpretation workstation software market, workstation-based seismic interpretation systems offer tools for generating various attributes.

Over the last decade or so, a growing trend adopted by software vendors has been to include as many interpretative techniques as possible, so that the seismic interpreter has access to all of them on his desktop. However, as this article illustrates, some of the processes such as acquisition footprint removal, structure-oriented filtering, and robust dip-steering options, may still be better handled by processing centres, especially when using some of the sophisticated and proprietary algorithms that are designed to run on clusters rather than workstations. Finally, the experience that processing analysts need to gain in the choice of parameterization for attribute computation is more easily learnt in processing centres. Though parameterization for attribute computation on workstations is a growing reality, interpreters may still need to rely on processing centres for receiving optimally processed data to carry out meaningful interpretations.

References

Al-Bannagi, M., Fang, K., Kelamis, P.G. and Douglass, G.S. [2005] Acquisition footprint suppression via the truncated SVD technique: case studies from Saudi Arabia. *The Leading Edge*, **24**, 832-834.

Budd, A.J.L., Hawkins, K., Mackewn, A.R. and Ryan, J.W. [1995] Marine geometry for optimum 3D seismic imaging. *57th EAGE Conference and Exhibition,* Expanded Abstracts, B030.

Chopra, S. and Larsen, G. [2000] Acquisition footprint — its detection and removal. *CSEG Recorder*, **25**(8), 16-20.

Cvetkovic, M., Falconer, S., Marfurt, K.J. and Perez, S.C. [2007] 2D stationary wavelet-based acquisition footprint suppression. *77th SEG Annual Meeting*, Expanded Abstracts, 2590-2593.

Done, W.J. [1999] Removal of interference patterns in seismic gathers. In: Kirlin, R.L. and Done, W.J. (Eds.), *Covariance Analysis for Seismic Signal Processing*. SEG, Tulsa, Geophysical Developments **8**, 185-225.

Drummond, J.M., Budd, A.J.L. and Ryan, J.W. [2000] Adapting to noisy 3D data – attenuating the acquisition footprint. *70th SEG Annual Meeting*, Expanded Abstracts, 9-12.

Fomel, S. [2002] Application of plane-wave destruction filters. *Geophysics*, **67**, 1946-1960.

Gersztenkorn, A., and Marfurt, K.J. [1999] Eigenstructure based coherence computations as an aid to 3-D structural and stratigraphic mapping. *Geophysics*, **64**, 1468-1479.

Gulunay, N., Sudhaker, V., Gerrard, C. and Monk, D. [1993] Prediction filtering for 3-D poststack data. *63rd SEG Annual Meeting*, Expanded Abstracts, 1183-l186.

Gulunay, N. [1999] Acquisition geometry footprints removal. *69th SEG Annual Meeting*, Expanded Abstracts, 637-640.

Hoecker, C. and Fehmers, G. [2002] Fast structural interpretation with structure-oriented filtering. *The Leading Edge*, **21**, 238-243.

Jervis, M. [2006] Edge preserving filtering on 3D seismic data using complex wavelet transforms. *76th SEG Annual Meeting*, Expanded Abstracts, 2872-2876.

Linville, A.F. and Meek, R.A. [1995] A procedure for optimally removing localized coherent noise. *Geophysics*, **60**, 191–203.

Luo, Y., Higgs, W.G. and Kowalik, W.S. [1996] Edge detection and stratigraphic analysis using 3-D seismic data. *66th SEG Annual Meeting*, Expanded Abstracts, 324-327.

Luo, Y., al-Dossary, S. and Alfaraj, M. [2002] Edge-preserving smoothing and applications. *The Leading Edge*, **21**, 136-158.

Marfurt, K.J., Kirlin, R.L., Farmer, S.L. and Bahorich, M.S. [1998] 3-D seismic attributes using a semblance-based coherency algorithm. *Geophysics*, **63**, 1150-1165.

Marfurt, K.J. [2006] Robust estimates of reflector dip and azimuth. *Geophysics*, **71**, 29-40.

Marfurt, K.J., Scheet, R.M., Sharp, J.A. and Harper, M.G. [1998] Suppression of the acquisition footprint for seismic sequence attribute mapping. *Geophysics*, **63**, 1024-1035.

Moldoveanu, N., Ronen, S. and Mitchell, S. [1999]. Footprint analysis of land and TZ acquisition geometries using synthetic data. *69th SEG Annual Meeting*, Expanded Abstracts, 641-644.

Randen, T., Monsen, E., Signer, C., Abrahamsen, A., Hansen, J., Saeter, T. and Schlaf, J. [2000] Three-dimensional texture attributes for seismic data analysis. *70th SEG Annual Meeting*, Expanded Abstracts, 668-671.

Soubaras, R. [2002] Attenuation of acquisition footprint for non-orthogonal 3D geometries. *72nd SEG Annual Meeting*, Expanded Abstracts, 2142-2145.

Walker, C.D.T., Mackewn, A.R., Budd, A.J.L. and Ryan, J.W. [1995] Marine 3D geometry design for optimum acquisition system response. *57th EAGE Conference and Exhibition*, Expanded Abstracts, B029.

Received 8 April 2008; accepted 7 July 2008.